Removal of sulfide from aqueous solution with transition metals ion impregnated clinoptilolite: characteristics, equilibrium, kinetic and thermodynamic approach

Sh. Karimi, A. Azadmehr*

Department of Mining & Metallurgical Engineering, Amirkabir University of Technology, 424 Hafez Avenue, Tehran 1875-4413, Iran, Tel. 00989124195819; email: A_azadmehr@aut.ac.ir (A. Azadmehr), Tel. 00989182802317; email: karimighale@aut.ac.ir (Sh. Karimi)

ABSTRACT

In this study, natural zeolite (clinoptilolite) was modified by Fe(III), Fe(III)–Ag(I) and Ag(I)–Cu(II) salts. Natural zeolite (obtained from Semnan area in the center of Iran) and modified zeolites were characterized by X-ray diffraction, X-ray fluorescence, scanning electron microscope, and Fourier transform infrared spectroscopy. The adsorption isotherm was studied with different adsorption isotherm models, namely Langmuir, Freundlich, Temkin and Dubinin–Radushkevich (D–R) models, and the constant values of these models were determined. This data displayed that sulfide adsorption onto Fe–Ag–zeolite and Ag–Cu–zeolite was performed favorably as a monolayer adsorption in homogeneous condition with a physical interaction. The homogeneous and heterogeneous adsorption contributes to sulfide adsorption onto Fe–zeolite, which occurs in a chemical absorption ion-exchange process. The maximum adsorption capacity of sulfide for Fe–zeolite, Fe–Ag–zeolite and Ag–Cu–zeolite are 4.69, 11.76 and 8.65 mg/g, respectively. In order to find the mechanism of adsorption, the reaction-based models (pseudo-first order and pseudo-second order) and diffusion-based models (intraparticle diffusion) are investigated. It can be calculated that the adsorption mechanism is controlled by sulfide ion concentration and the number of active sites on the surface of modified zeolites. Thermodynamic studies indicate that sulfide adsorption onto Fe–zeolite was exothermic and spontaneous but for Fe–Ag–zeolite and Ag–Cu–zeolite adsorbents were endothermic and spontaneous.

Keywords: Zeolite; Sulfide; Adsorption; Isotherm model; Kinetic; Thermodynamic

1. Introduction

Nowadays, the rapid development of the mining activities, the industrial processes and petroleum refining have caused the generation of undesirable toxic pollutants from sulfur compounds, such as mercaptans (RSH), organosulfur (R_2S), disulfides (RSSR), thiophenes, Hydrogen sulfides (H_2S) and sulfide (S^{2-}) whose hazardous effects on the quality of drinking water have increased considerably. One of the major species of sulfur compounds is sulfide ion (S^{2-}), which can be liberated from H_2S and HS^- into the environment. These compounds are odorous, corrosive and toxic. Nowadays, desulfuration from fuel cells has attracted attention considerably [1,2]. If the concentration of sulfides (S^{2-}) ions in drinking water is more than 10 ppm, it is surely harmful to human health. Therefore, it must be removed from industrial wastewaters before releasing to the environmental. Thus, over the past decades, many different physicochemical methods such as ion exchange [3], oxidation [4], chemical precipitation [2], biological [5] and electrochemical have been used [6,7].

The abovementioned methods have been applied to remove different species of sulfur compounds from aqueous solutions by synthesized and natural adsorbent [8,9] because they are easy handling, economical and efficient relative to other physicochemical methods. Zeolite Y, Zeolite A and

* Corresponding author.

clinoptilolite (natural zeolite) can be suitable adsorbents to remove pollution environmental, which are summarized in Table 1 [9–18].

Zeolites are hydrated aluminosilicates consisting of a three-dimensional framework of SiO_4 and AlO_4 tetrahedra. The basic structure of the zeolite crystal contains three types of channels of tetrahedral rings, including eight and ten tetrahedral rings, which grow at different directs [19]. The substitution of silicon by aluminium elements leads to a negative charge of the framework. It is neutralized by monovalent, divalent or trivalent cations in the crystal structural such as Ca, Mg^{2+}, Na^+, K^+, etc. The fundamental of ion exchange in zeolites is replaced by these cations, which are within tetrahedral rings channel [20].

In order to adsorb anion ions onto zeolite, the surface of anion ions must be changed to a positive charge; therefore, using organic compounds and surfactant as a modifier of the surface of zeolites has been well known [21,22]. The adsorptive desulfurization with natural and synthesized zeolite has been proposed by ion-exchange mechanism [23]. Of course, modified zeolite surface with transition metals can adsorb organosulfur compounds selectively and competitively [24]. These properties coordinate directly through a sulfur metals in cavities of zeolite structures based on the π-complexation mechanisms [25].

As mentioned above, the literature survey shows (as seen in Table 1) that zeolite is one of the significant adsorbents to remove and to separate sulfur compounds from aqueous solution, organic solvents and oil.

Table 1
A summary of sulfur compounds adsorption onto various adsorbents

Adsorbent	Kind of investigation	Adsorbed material	Reference
Rice husk	Isotherm and kinetic studies	Sulfide (1.7 mg/g)	[9]
Fibrillated cellulose	Isotherm	Sulfide (–)	[10]
Y zeolite	Infrared spectroscopy	Benzothiophene (20 mg/g)	[11]
Clinoptilolite	Characterization and optimum conditions	H_2S (30 mg/g)	[12]
Andisols	Isotherm and kinetic studies	SO_4^{2-} (15.36 mg/g)	[13]
Clinoptilolite	Isotherm and kinetic studies	SO_2 (200 mg/g)	[14]
Andisols	Isotherm and kinetic studies	SO_4^2 (24 mg/g)	[15]
Y zeolite	Isotherm and kinetic studies	Sulfur (–)	[16]
Clinoptilolite	Characterization and optimum conditions	H_2S (1.39 mg/g)	[17]
Organo-nano-clay	Isotherm and kinetic studies	SO_4^{2-} (21.5 mg/g)	[18]

Clinoptilolite is a significant type of natural zeolite, which is a well-known appropriate adsorbent for removing environmental pollution of heavy metals from wastewater and industrial effluent [20]. Although the application of modified clinoptilolite as sulfide adsorbent is not considered well, the impregnation of zeolite surface using metal salts was known as a route map to remove anion ions [26]. Therefore, the objectives of this study are as follows:

- to investigate the ability of modified Iranian natural zeolite (clinoptilolite) to remove sulfide from aqueous solution;
- to perform equilibrium study of sulfide adsorption by modified zeolite for characterization of the process and to find the best model to describe the sulfide adsorption mechanism; and
- to find thermodynamic parameters (Gibbs free energy, standard enthalpy and standard entropy) and to determine the kinetic model and find the mechanism of sulfide adsorption.

2. Materials and methods

2.1. Materials

A representative sample was obtained from Semnan province mine in the center of Iran. This sample was fully crushed until to obtain the nominal particle size fractions of –150 μm in diameter. All chemical compounds were purchased from Merck Company (Germany) and used without further purification.

2.2. Physical measurements

X-ray diffraction (XRD) spectra were obtained using a Philips X-ray diffractometer 1140 (α = 1.54 A, 40 kV, 30 mA, calibrated with Si-standard) and a Philips X-ray diffractometer X unique II (80 kV, 40 mA, calibrated with Si-standard), respectively. Infrared spectra from 4,000 to 400 cm^{-1} were recorded on a Shimadzu 470 FT-IR instrument, using KBr pellets. Fourier transform infrared (FTIR) spectroscopy has been used for chemical functional groups. The specific surface area was measured by N_2 adsorption 77 K using Brunauer–Emmett–Teller method.

2.3. Modification of zeolite

To obtain the most appropriate modified zeolite by transition metals for removing sulfide, 5.5 g of zeolite in 0.1 mol/L solution (75 mL) of some of transition metal nitrate, acetate, chloride and sulfate solutions, which were prepared with distillation water, were suspended for overnight at room temperature, and then solid phase was separated by centrifuge and dried at room temperature for 24 h and was crushed and sieved to –150 μm in diameter as can be seen in Table 2. The ability of modified zeolites to adsorb sulfide ion has been studied, and the obtained results are displayed in Table 2.

2.4. Equilibrium isothermal models

The maximum adsorption capacity of sulfide, surface properties of modified zeolite and mechanism of adsorption

process were characterized using four different isotherm models, which include two-parameter models, namely Langmuir, Freundlich, Temkin and Dubinin–Radushkevich (D–R). The experiments were conducted with sulfide concentration of 100, 250, 500, 750, 1,000 and 1,500 mg/L at 25°C, the stirring speed of 500 rpm, solid to liquid ratio (S/L) of 0.05, pH of 11.5 and a particle size of –150 μm. The linear equations of Langmuir, Freundlich, Temkin and D–R are listed in Table 3. In order to evaluate reversibility or irreversibility of adsorption in the homogenous process, a dimensionless constant called separation factor R_L (also known as equilibrium parameter) is presented by the following equation [27,28]:

$$RL = \frac{1}{1 + b \times C_0} \qquad (1)$$

where C_0 (mg/L) and b (L/mg) are the initial S^{2-} concentration, respectively, and Langmuir constant is related to the energy of adsorption. The values of R_L express that if $R_L > 1$, $R_L = 0$, $R_L = 1$ and $0 < R_L < 1$, the adsorption will be unfavorable, irreversible, linear and favorable, respectively [29]. The Marquardt's percent standard deviation (MPSD) value between the experimental and calculated q_e values is given as [30]:

$$MPSD = 100 \sqrt{\frac{1}{n_m - n_p} \sum_{i=1}^{n} \left(\frac{\left(\sum_{i=1}^{N} q_{e,i,\exp}\right) - \left(\sum_{i=1}^{N} q_{e,i,\text{cal}}\right)}{\sum_{i=1}^{N} q_{e,i,\exp}} \right)_i^2} \qquad (2)$$

2.5. Kinetic studies

For the kinetic investigation, 5 g of modified zeolites were suspended in 100 mL of sulfide at various initial

Table 2
Absorption rate after the addition of modifier (conditions: particle size: –150 μm, stirrer speed: 500 rpm, 298 K temperature, pH: 11.5, amount of zeolite: 5.5 g, initial concentration of sulfide: 1,000 mg/L, solid:liquid (S:L): 0.05)

Sulfide adsorption (%)	Name of modifiers	Type of modifier
37.5	$Fe(NO_3)_3$	Nitrate
19.8	$Ni(NO_3)_2$	
36.4	$Cu(NO_3)_3$	
0.08	KNO_3	
33.5	$AgNO_3$	
0.14	$Cd(NO_3)_2$	
0.01	$Co(NO_3)_2$	
0.12	$Mn(NO_3)_3$	
15.3	$FeSO_4$	Sulfate
–	Na_2SO_4	
0.02	$ZnSO_4$	
0.03	CH_3COONH_4	Acetate
30	$BaCl_2$	Chloride
0.29	NaCl	
–	$CaCl_2$	
–	NH_4Cl	
–	–	Raw zeolite

Table 3
Linear isotherm equations of different isotherm models

Model	Linear equation	Descriptions	Reference
Langmuir	$\dfrac{C_e}{q_e} = \dfrac{1}{b \times Q_m} + \dfrac{C_e}{Qm}$	q (mg/g): amount of adsorbed metal ion per unit weight of adsorbent; C_e (mg/L): metal ion concentration in solution at equilibrium (after adsorption); b (L/mg): the Langmuir isotherm constants; Q_m: adsorption capacity, maximum in monolayer adsorption	[36,37]
Freundlich	$\log q_e = \log K_f + \dfrac{1}{n} \log C_e$	K_F ($mg^{1-1/n}$ $L^{1/n}$ g^{-1}): Freundlich constants which display adsorption capacity of the zeolite; n (g/L): Freundlich constants which represent adsorption intensity (or surface heterogeneity) of the adsorbent	[38]
Temkin	$q_e = \dfrac{RT}{b} \ln A + \dfrac{RT}{b} \ln C_e$	b (J/mol): Temkin isotherm constants that related to the heat of adsorption; A: Temkin isotherm constants; R: the gas constant (8.314 J/mol K); T: The absolute temperature	[42,43]
Dubinin–Radushkevich	$\ln q_e = \ln q_{max} - \beta \varepsilon^2$ $\varepsilon = RT \ln(1 + 1/C_e)$ $E = \dfrac{1}{\sqrt{2\beta}}$	q_{max} (mg/g): capacity maximum of adsorption; β (mol^2/KJ^2): a constant related to adsorption energy; E: free energy per molecule of adsorbate (KJ), which represent: if $E < 8$ kJ/mol: physical adsorption; If $8 < E < 16$ kJ/mol: chemical absorption or ion-exchanges; for $E > 16$ kJ/mol: particle diffusion governs the reaction	[44,45]

concentrations of 100, 250, 400, 500, 750, 1,000, 1,500 and 2,000 mg/L. Each experiment was conducted at different time intervals (10, 20, 30, 45, 60 and 90 min) to determine the period required to reach the adsorption equilibrium and maximum removal of sulfide. The sulfide adsorption mechanism onto modified zeolites was evaluated by pseudo-first-order, pseudo-second-order and intraparticle diffusion models (Table 4).

2.6. Thermodynamic study

Thermodynamic experiments were carried out by placing 2 g adsorbents (Fe–zeolite, Fe–Ag–zeolite and Ag–Cu–zeolite) in a beaker containing 100 mL of sulfide solution 1,000 mg/L at 40 min contact time with various temperatures (298, 303, 313 and 323 K). Thermodynamic parameters can be explained by the following equations [31]:

$$q_e m = V(C_0 - C_e) \tag{3}$$

$$K_d = \frac{q_e}{C_e} \tag{4}$$

where q_e is the equilibrium adsorption capacity of sulfide (mg/g); C_0 is the initial sulfide concentration (mg/L); C_e is the equilibrium of sulfide concentration in solution after Fe, Fe/Ag and Cu/Ag absorbed by zeolite (mg/L); m is the mass of zeolite used (g); and V is the volume of solution (L). The K_d values are used in the following equation to determine the Gibbs free energy of sorption process at different temperatures.

$$\Delta G° = -RT\text{Ln}K_d \tag{5}$$

where $\Delta G°$ is the free energy of Ni adsorption (kJ/mol); R is the universal gas constant (8.314 J/mol K); and T is the temperature (K) of solution during the adsorption process. The adsorption distribution coefficient may be expressed in terms of enthalpy change ($\Delta H°$) and entropy change ($\Delta S°$) as a function of temperature:

$$\text{Ln}K_d = \frac{\Delta S°}{R} - \frac{\Delta H°}{RT} \tag{6}$$

where $\Delta H°$ is the heat of adsorption (kJ/mol), and $\Delta S°$ is the standard entropy change of adsorption (kJ/mol) [32,33].

3. Results and discussion

3.1. Modification of zeolite

The modification of zeolite with transition metal salts show:

- Among the metal salt used as the modifier surface of zeolite, the nitrates salts caused the highest maximum of sulfide adsorptions relative to other anion polarities such as sulfate and acetate. The low adsorption affinity to NO_3^{3-} on zeolite surfaces is attributed to the relative small ionic negative charge of nitrate.
- As seen in Table 2, the used mixture of two salt metals ($Fe(NO_3)_3$–$AgNO_3$ and $AgNO_3$–$Cu(NO_3)_2$) as modifier caused considerable improvement in sulfide uptake on modified zeolite in comparison with other modifier salt metals alone. With respect to the transition metal cobalt, manganese and cadmium sulfides create insoluble salts; thus, it is expected that this modified zeolite caused adsorption uptake of sulfide, but it does not make a difference in the absorption quantity. Other modifiers such as iron, copper and silver can enhance the adsorption of sulfide. These results show that the interaction between metal ions with zeolite structure is more significant than that of metal ions and sulfide.
- Alkali and alkaline earth elements except barium had no significant effect on sulfide uptake. In other words, transitional metals impregnated in zeolite cavities have much effect on sulfur capture.
- The increase of sulfide absorption using transition metal salts as modifier area follows as:
  Fe(III) > Cu(II) > Ag(I) > Ni(II) > Fe(II) >>> Co(II) ~ Cd(II) ~ Mn(II) ~ Zn(II).

The value of solubility product (K_{sp}) constant of these transition metal sulfide follows this sequence [34]: MnS > NiS > FeS > CoS > ZnS > CdS > CuS > Ag_2S >> Fe_2S_3.

With respect to this sequence modifier, Fe(III) > Cu(II) > Ag(I) ions with the least value of solubility product constant (K_{sp}) caused a significant improvement in the adsorption of sulfide compared with the other transition metals. On the other hand, whatever the value of solubility product constant

Table 4
Kinetic equations of different kinetic models

Model	Linear equation	Description	Reference
Pseudo-first-order equation	$\ln(q_e - q_t) = \ln q_e - K_1 t$	q_t: amounts of Ions adsorbed after t units of time; q_e: amounts of Ions adsorbed after time of reach to equilibrium (mg/g); k_1: the pseudo-first-order rate constant for the adsorption process (min^{-1}).	[38,46]
Pseudo-second-order equation	$\frac{t}{q_t} = \frac{1}{K_2(q_e)^2} + \frac{1}{q_e}t$	k_2: the equilibrium rate constant of the pseudo-second-order equation (g/mg min)	[47,48]
Intra-particle diffusion equation	$q_t = K_i t^{\frac{1}{2}}$	K_i: the intraparticle diffusion rate constant (mg/(g min$^{1/2}$))	[42,47]

(K_{sp}) of metal sulfide is less (the metal as modifier agent for sulfide adsorption), the uptake of sulfide on modified zeolite is enhanced.

3.2. Characterization of zeolite

XRD and X-ray fluorescence (XRF) were used to study mineralogy and chemical elemental analysis of the raw and modified zeolites. The XRD patterns of raw zeolite, Fe–zeolite, Fe–Ag–zeolite and Ag–Cu–zeolite samples are shown in Fig. 1. The XRD patterns of raw zeolite show the major diffraction with highest intensities relevant to planes (400) and (020) whose basal spacing of different planes (d_{hkl}) are 3.89 and 8.61 Å, respectively [35]. This result indicates that the main mineral of this zeolite type contains clinoptilolite with minor contents of mica-illite, dolomite and feldspars as impurities. According to the chemical composition of this sample (XRF results in Table 5), silica oxide to aluminum oxide ratio (SiO_2/Al_2O_3) is more than 5. It confirms that this sample (zeolite obtained from Semnan area) mainly consists of clinoptilolite.

The basal spacing of planes did not change considerably by modifying treatment only the basal spacing $d_{(020)}$ decreased using $Fe(NO_3)_3$–$Ag(NO_3)$ modifier agent.

According to Table 6, the value changes of the 2θ diffraction of planes (400) and (020) for Fe–Ag–zeolite after modifying are 0.36 and 1.36 Å, respectively. As seen in Table 6, the relative intensity of plane (020) for raw zeolite decreased after loading transition metal on the surface of zeolite.

However, the XRD patterns of modified zeolite in comparison with those of raw zeolite showed the modification treatment did not lead to significant crystalline structure changes; however, the surface of zeolite was affected by transition metal elements. It is obvious that the transition metals (Fe(III), Ag(I) and Cu(II) ions) impregnated the surface of zeolite as a modifier. This occurrence was known well in catalyst reaction [35]. As seen in Table 5, the XRF result confirms the considerable presence of Fe, Fe–Ag and Ag–Cu in Fe–zeolite, Fe–Ag–zeolite and Ag–Cu–zeolite, respectively.

The FTIR spectroscopy of raw and modified zeolites were used to describe their functional groups and characterization of atomic bonding. Infrared spectra of the raw zeolite, Fe–zeolite, Fe–Ag–zeolite and Ag–Cu–zeolite are illustrated in Fig. 2. The stretching bands at 3,630 and 3,443 cm^{-1} indicates O–H bond linkage of a hydroxyl group, which has an interaction with ions (Si–OH, Al–OH) and O–H of water molecule within the crystal structure of zeolite, respectively. This broad-stretching band is due to hydrogen bonding between hydrogen and oxygen of different water molecules [11]. The relative broadband at 1,632 cm^{-1} relates to H–O–H bending band. The broadband with a high density is observed at 1,067 cm^{-1} indicates Si–O–Si, Al–O–Si
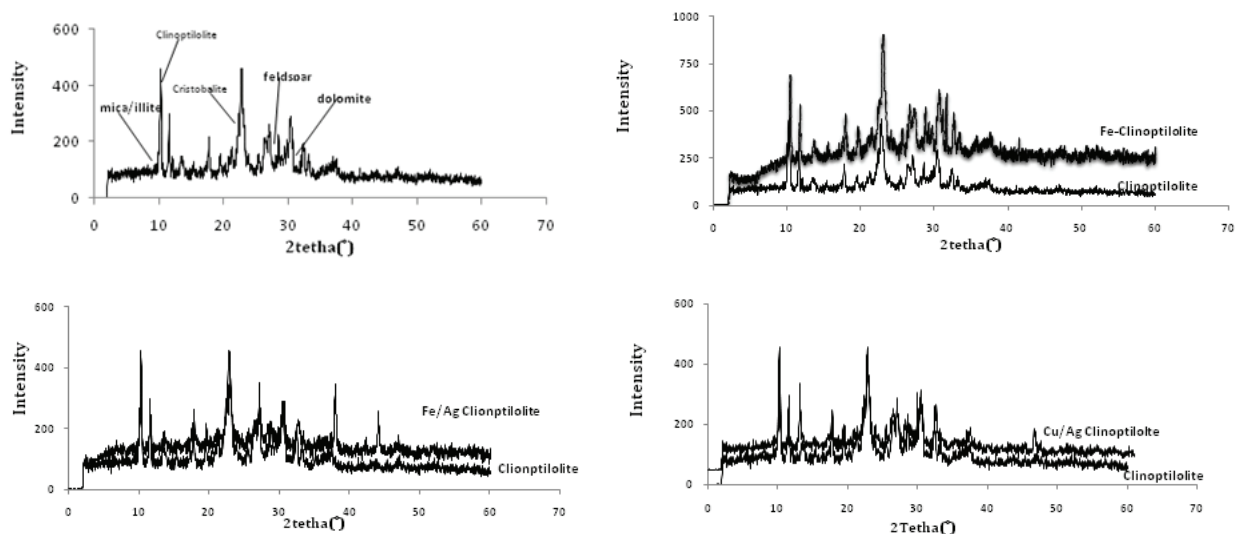

Fig. 1. XRD pattern of raw zeolite, Fe–zeolite, Fe–Ag–zeolite and Ag–Cu–zeolite.

Table 5
Chemical analysis of raw zeolite sample (XRF data)

Sample	L.O.I	Na$_2$O	MgO	Al$_2$O$_3$	SiO$_2$	SO$_3$	K$_2$O	CaO	Fe$_2$O$_3$	Ag$_2$O	CuO
Raw	11.6	3.12	0.60	10.93	66.29	0.461	3.979	1.94	0.84	–	–
Fe–zeolite	17.30	3.33	0.51	8.39	53.6	0.44	2.8	0.98	12.45	–	
Fe–Ag–zeolite	18.3	1.98	0.44	6.8	50.56	0.41	1.27	0.57	10.9	10.33	
Ag–Cu–zeolite	17.95	1.55	0.36	4.90	48.08	0.34	1.33	0.48	0.45	12.14	11.56

Note: L.O.I. – loss on ignition.

and Al–O–Al asymmetrical stretching bands, which are overlapped with others. The bending vibration of Si–O–M (M: Na, k and Ca) is observed at 607 cm^{-1}. The bending vibration bands at 795 cm^{-1} are concerned to Si–O–Si of Quartz as an impurity in the zeolite. According to Table 7, the values of stretching and bending of fundamental groups of modified zeolite relative to raw zeolite did not change considerably by using transition metals as modifier agents. This result emphasized that the surface of zeolite was impregnated by transition metals.

The specific surface area for raw zeolite, Fe–zeolite, Fe–Ag–zeolite and Ag–Cu–zeolite are 33, 56, 94 and 79 m^2/g, respectively. These results indicate Fe–Ag–zeolite is more proper for sulfide adsorption.

Table 6
The basal spacing of diffraction planes of raw and modified zeolite

Sample	Plane	2θ (°)	Intensity	d (Å)
Raw zeolite	020	10.27	798	8.61
Raw zeolite	400	22.82	1,000	3.89
Fe–zeolite	020	10.21	597	8.66
Fe–Ag–zeolite	020	11.63	642	7.60
Fe–Ag–zeolite	400	22.95	1,000	3.87
Ag–Cu–zeolite	400	23.18	1,000	3.83

Scanning electron microscope (SEM) images of raw zeolite, Fe–Ag–zeolite and Fe–Ag–zeolite after adsorption are presented in Figs. 3(a)–(c), respectively. It is obvious from Fig. 3(a) that the porous matrix of raw zeolite surface are 8–10 nm on which particles having size 300–500 nm have aggregated. The particle size distribution of Fe–Ag–zeolite obviously changed after impregnating by Fe(III) and Ag(I) ions. As seen in Fig. 3(c), the change of morphology of Fe–Ag–zeolite surface after adsorption has confirmed the sulfide adsorption process onto the surface of Fe–Ag–zeolite. These properties were observed exactly for Fe–zeolite and Ag–Cu–zeolite.

3.3. Adsorption isotherm models

In the adsorption processes, the adsorption capacity, surface properties, mechanism of adsorption and affinity of the adsorbents were investigated by equilibrium concentration adsorbate (sulfide ions) in solution, and the amount of modified adsorbent (zeolite) and adsorbate (sulfide ions). In this study, four different isotherm models (Langmuir, Freundlich, Temkin and D–R isotherm models) were examined.

3.3.1. Langmuir isotherm

The obtained data of sulfide adsorption at various initial concentrations of sulfide were applied to the Langmuir isotherm model showing the plot of the linear form of Langmuir with a correlation coefficient (R^2) 0.990, 0.998 and 0.944 for
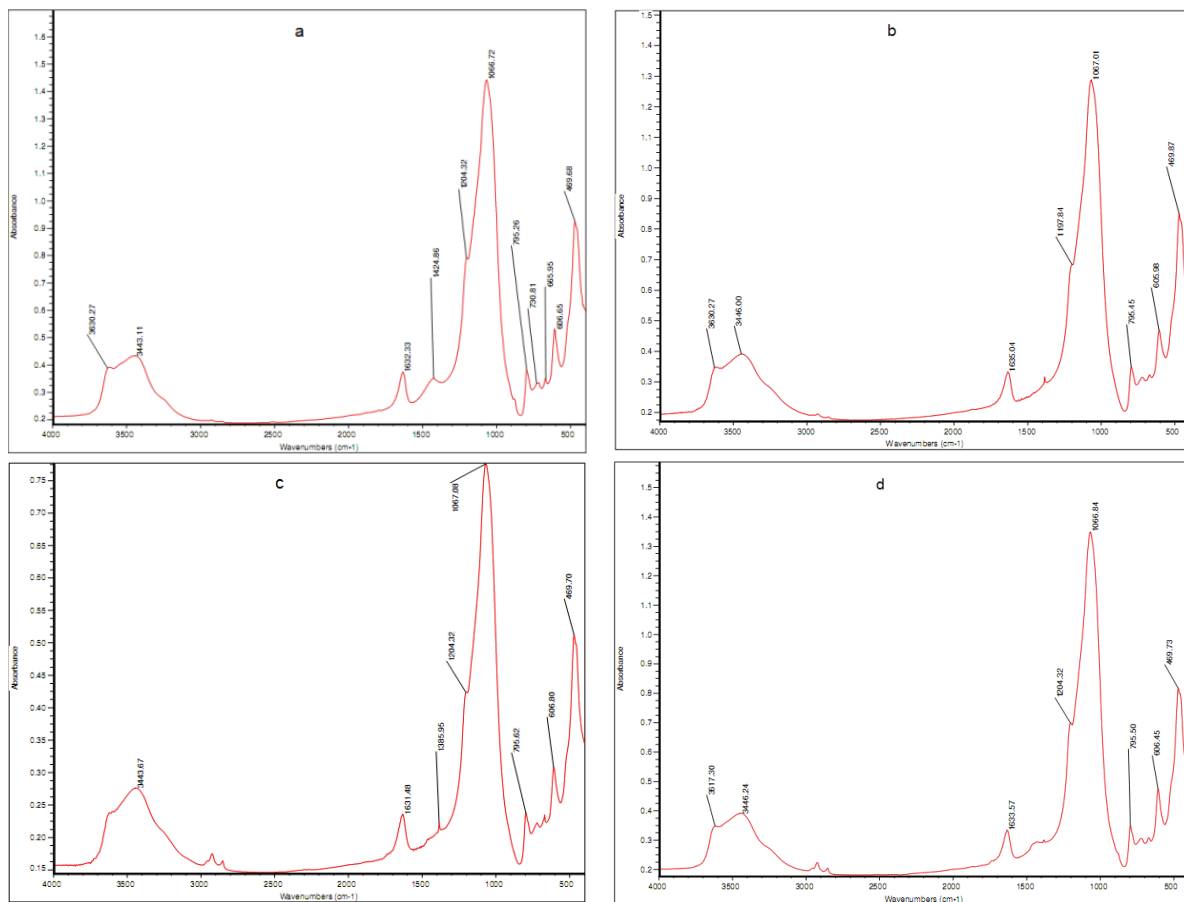

Fig. 2. FTIR pattern of (a) raw zeolite, (b) Fe–zeolite, (c) Fe–Ag–zeolite and (d) Ag–Cu–zeolite.

Fe–zeolite, Fe–Ag–zeolite and Ag–Cu–zeolite, respectively. The magnitude of standard deviation (S.D.) and R_L confirmed that adsorption data for sulfide removal best fitted the Langmuir for Fe–zeolite and Fe–Ag–zeolite composites. Therefore, the range of separation factor (R_L) for modified zeolite modified by Fe(NO$_3$)$_3$, Fe(NO$_3$)$_3$–AgNO$_3$ and AgNO$_3$–Cu(NO$_3$)$_2$ are 0.0407–0.3891, 0.6812–0.17609 and 0.1602–0.6561, respectively. This data indicates that sulfide adsorption onto modified zeolite in different sulfide concentrations (especially in high initial sulfide concentration) is favorable and reversible because R_L values are between 0 and 1. These results suggest that sulfide uptake occurs on the homogenous surface of Fe–zeolite, and Fe–Ag–zeolite by monolayer adsorption of sulfide without interaction between adsorbed sulfide ions. The maximum adsorption capacity (Q_m) of modified zeolites (from Semnan area of Iran) according to Langmuir model follows this order: Fe–Ag–zeolite > Ag–Cu–zeolite > Fe–zeolite. Of course, adsorption of sulfide toward Ag–Cu–zeolite was not described very well by Langmuir isotherm though the highest value of binding energy relates to Ag–Cu–zeolite composite [36,37].

3.3.2. Freundlich isotherm

In order to study multilayer adsorption of sulfide onto modified zeolite, fitting the experimental data with Freundlich isotherm model was plotted as $\log q_e$ vs. $\log C_e$. With respect to correlation coefficient (R^2) and S.D. values, sulfide adsorption from aqueous solutions by Fe–Ag–zeolite is satisfactorily described by Freundlich isotherm model but adsorptive behavior of sulfide onto Fe–zeolite and Ag–Cu–zeolite was not described well by Freundlich model although the empirical constant n, which relates to adsorption intensity (surface heterogeneity) for all modified zeolites, is favorable because based on literature survey if $1 < n < 10$, the adsorption process is favored. The values of Freundlich constants and R^2 are listed in Table 8.

This occurrence indicates that at the beginning of sulfide adsorption process, the stronger binding sites are occupied, and non-uniform distribution of adsorption energy are observed as exponential reduction [28,32,38]. The K_F (adsorption capacity) value of sulfide adsorption onto Fe–Ag–zeolite in comparison with other anion adsorption onto mineral adsorption is considerable [39].

3.3.3. Temkin isotherm

Temkin isotherm model modified the Langmuir model by considering temperature in adsorption processes [40]. It was assumed that the binding energies of interactions between modified zeolites and sulfide ions are distributed onto zeolite surface uniformly, which causes the linear decrease in the energy of adsorption.

According to Temkin isotherm model, the linear plot of q_e vs. $\log C_e$ for different modified zeolites at temperature 298 K was obtained. The experimental data of sulfide adsorption onto Fe–Ag–zeolite and Ag–Cu–zeolite fitted well with R^2 and S.D. values 0.994–0.05 and 0.985–0.07, respectively. The values of parameter b, which relate to the energy of adsorption, are 1.03 and 0.86 kJ/mol for Fe–Ag–zeolite and Ag–Cu–zeolite, respectively. With respect to b (Temkin isotherm constant) values that are <8 kJ/mol, which indicates sulfide adsorption onto these adsorbents is a physisosorption process [40,41]. In other words, the interaction between sulfide ion and surface of Fe–Ag–zeolite and Ag–Cu–zeolite is a weak process. The investigation of experimental data of sulfide adsorption
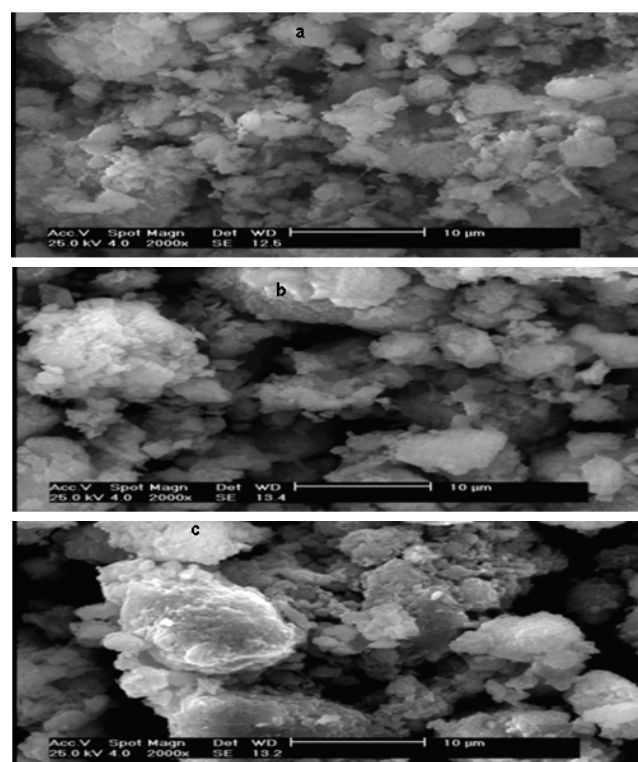
Fig. 3. SEM images at 2,000× for (a) raw zeolite, (b) Fe–Ag–zeolite and (c) Fe–Ag–zeolite after sulfide adsorption.

Table 7
The values of starching and bending of fundamental groups of modified zeolite relative to raw zeolite

Assignment	Raw zeolite samples (cm^{-1})	Fe–zeolite samples (cm^{-1})	Fe–Ag–zeolite samples (cm^{-1})	Ag–Cu–zeolite samples (cm^{-1})
$\sqrt{}$(Si–OH,Al–OH)	3,630	3,630	3,635	3,617
$\sqrt{}$(H–O–H)	3,443	3,446	3,443	3,446
ᵟ(H–O–H)	1,632	1,635	1,631	1,633
$\sqrt{}$(Si–O–SiO2)	795	795	795	795
ᵟ(Al–O–Si)	469	469	469	469
ᵟ(Si–O–Si)	1,066	1,067	1,067	1,066

onto Ag–Cu–zeolite reveals that Temkin model (modified Langmuir model) could well describe this process [42,43]. The values of Temkin constants and R^2 are listed in Table 8.

3.3.4. Dubinin–Radushkevich (D–R) isotherm

In order to further find the mechanism involved in the sulfide adsorption onto the surface of modified zeolites, the linear form of $\log q_e$ vs. $\text{Ln}^2(1 + c^{-1})$ must be primarily found. The parameters q_m and B of empirical D–R isotherm model are calculated from the intercepts and slopes, respectively. As seen in Table 8, the magnitude of free energy of sulfide adsorption (E) for Fe–Ag–zeolite, Ag–Cu–zeolite and Fe–zeolite are 10.00, 7.451 and 7.071 kJ, respectively. These calculated values of E (free energy of adsorption) indicate sulfide adsorption by Fe–zeolite occurred through chemical absorption ion-exchange process, and sulfide adsorption by Fe–Ag–zeolite and Ag–Cu–zeolite occurred through a physical process [44,45].

3.3.5. Evaluation of adsorption isotherm models of sulfide onto modified zeolites

In this study, four isotherms models, including Langmuir, Freundlich, Temkin and D–R, were used to analyze the experimental data of sulfide adsorption onto modified zeolites.

Based on the high correlation coefficient (R^2) and low S.D., the best fitting results for Fe–zeolite and Ag–Cu–zeolite are attributed to Langmuir and Temkin isotherm models, respectively. These adsorption processes led to a homogeny and monolayer with an infinite number of adsorption sites. Furthermore, Langmuir, Freundlich and Temkin isotherm have fitted favorably to experimental data for Fe–Ag–zeolite with the correlation coefficient (R^2) more than 0.990. This phenomenon shows the complexity treatment of involving sulfide ions and surface of Fe–Ag–zeolite. It seems the homogeneous

and heterogeneous adsorption can be predominated in sulfide adsorption onto Fe–Ag–zeolite. The maximum adsorption capacities of sulfide for Fe–zeolite, Fe–Ag–zeolite and Ag–Cu zeolite are 4.69, 11.76 and 8.65 mg/g, respectively. These results in comparison with those of other reports are considerable [9,10]. According to Temkin and D–R isotherm models, the main mechanisms controlling sulfide adsorption on Fe–zeolite, Fe–Ag–zeolite and Ag–Cu–zeolite are chemical absorption ion-exchange process and physical process, respectively.

3.4. Evaluation of adsorption kinetic model of sulfide onto zeolite

Based on plots of Fig.4 the different parameters' values of each model are calculated from the linear equation and are presented in Table 9.The highest correlation coefficient (R^2) values (>0.990) and lowest S.D. values (<0.090) relate to a pseudo-second-order kinetic model for describing the experimental results at different initial sulfide. Results (Table 9) have confirmed greatly that the rate of adsorption sulfide and adsorption mechanism is controlled by sulfide ion concentration and the number of active sites on the surface of modified zeolites. In order to determine the rate-controlling step on sulfide adsorption process by mechanism mass transfer, the intraparticle diffusion has been investigated. According to S.D. and regression coefficients (R^2) of this model for Fe–zeolite, and Fe–Ag–zeolite, in high sulfide, initial concentration, the rate of adsorption process can be controlled relatively by diffusion model. Of course, the main model that well describes the rate of sulfide adsorption onto modified zeolite is a pseudo-second-order kinetic model [46–48].

3.5. Thermodynamic study

In order to determinate thermodynamic parameters, according to Eq. (6), the values of $\Delta H°$ and $\Delta S°$ were

Table 8
Langmuir, Freundlich, Temkin and Dubinin–Radushkevich isotherm constants for sulfide adsorption

Model	Parameter	Fe–zeolite	Fe–Ag–zeolite	Ag–Cu–zeolite
Langmuir	q_m (mg/g)	4.690	11.764	8.658
	R^2	0.9900	0.9985	0.9444
	R_L	0.389–0.040	0.681–0.176	0.656–0.160
	b	0.015	0.004	0.005
	MPSD	0.1184	0.0068	0.1241
Freundlich	K_F ($\text{mg}^{1-1/n}\,\text{L}^{1/n}\,\text{g}^{-1}$)	3.227	6.934	14.368
	n (g/L)	2.330	1.482	1.286
	R^2	0.9340	0.9948	0.8954
	MPSD	0.1930	0.0090	1.528
Temkin	b (J/mol)	2,117.760	1,037.465	863.410
	A (L/mg)	7.954	16.751	40.397
	R^2	0.9418	0.9942	0.9855
	MPSD	0.5210	0.0095	0.031
Dubinin–Radushkevich	q_m (mg/g)	7,230.041	2,661.113	1,794.533
	b (mol^2/KJ^2)	5×10^{-9}	7×10^{-9}	10×10^{-9}
	E (KJ/mol)	10.000	8.451	7.071
	R^2	0.9532	0.9986	0.9585
	MPSD	0.1921	0.0069	0.0010

determined from the slopes and intercept of the plot of $\ln K_d$ vs. $1/T$. Table 10 demonstrates thermodynamic parameters for sulfide adsorption.

The negative value of $\Delta H°$ for Fe–zeolite adsorbent indicates that the adsorption process is exothermic; this means that increasing temperature causes a decrease in the amount of adsorbed sulfide. The negative value of entropy changes ($\Delta S°$) in adsorption process indicates associative mechanism because the adsorption process causes the number of ions in the solution to decrease [49]. Negative $\Delta G°$ values of sulfide adsorption onto Fe–zeolite at different temperatures indicate that this adsorption process is spontaneous.

As seen in Table 10, by analyzing the values of $\Delta H°$, $\Delta S°$ and $\Delta G°$ for Ag–Cu–zeolite and Fe–Ag–zeolite, it can be speculated that sulfide adsorption onto both adsorbents is endothermic, associative and spontaneous. The positive value of $\Delta H°$ (endothermic process) is an indicative of an increase in sulfide adsorption on the successive increase in temperature. The positive value of $\Delta S°$ demonstrates the increased randomness at the film interface (between solid and solution) during the fixation of the sulfide ion on the active sites on the surface of Ag–Cu–zeolite and Fe–Ag–zeolite [50].

The magnitude of standard enthalpy changes ($\Delta H°$) and standard entropy changes ($\Delta S°$) for Ag–Cu–zeolite and Fe–Ag–zeolite are considerable in comparison with these parameters for Fe–zeolite.

With the increase of the temperature, the degree of the spontaneity of the sulfide adsorption onto Fe–zeolite,

Table 9
Kinetic parameters for the adsorption of sulfide onto (a) Fe–zeolite, (b) Fe–Ag–zeolite and (c) Ag–Cu–zeolite

(a) Pseudo-first-order equation						(a) Pseudo-second-order equation				(a) Intraparticle diffusion equation		
C_0 (mg/L)	q (exp) (mg/g)	q_1 (mgs/g)	k_1 (min^{-1})	$(R_1)^2$	MPSD	q_2, (mg/g)	k_2 g/(mg. min)	$(R_2)^2$	MPSD	k_3 (mg/(g min$^{1/2}$))	$(R_3)^2$	MPSD
100	1.47	3.081	−0.05	0.3690	0.437	1.36	4.510	0.9909	0.052	0.062	0.5088	0.185
250	3.41	1.589	−0.03	0.6186	0.942	3.80	0.022	0.9880	0.104	0.275	0.8273	0.555
500	4.37	3.478	−0.03	0.9639	0.384	5.89	0.006	0.9941	0.086	0.343	0.9906	0.322
750	4.05	3.239	−0.03	0.9436	0.586	5.36	0.006	0.9991	0.018	0.274	0.9543	0.537
1,000	5.05	20.605	−0.08	0.8814	0.715	3.44	0.013	0.8623	0.141	0.643	0.9606	0.789

(b) Pseudo-first-order equation						(b) Pseudo-second-order equation				(b) Intraparticle diffusion equation		
C_0 (mg/L)	q (exp) (mg/g)	q_1 (mg/g)	k_1 (min^{-1})	$(R_1)^2$	MPSD	q_2 (mg/g)	k_2 g/(mg. min)	$(R_2)^2$	MPSD	K_3 (mg/(g min$^{1/2}$)]	$(R_3)^2$	MPSD
100	1.550	6.514	0.003	0.1747	0.531	1.347	1.655	0.9988	0.054	−0.071	0.1903	0.928
250	3.190	46.095	0.027	0.2951	0.995	3.053	0.664	0.9997	0.038	−0.054	0.2692	0.867
500	6.350	2.047	0.009	0.8461	0.545	4.968	0.042	0.9993	0.029	−0.208	0.9099	0.182
750	8.370	1.222	−0.004	0.1193	1.593	7.968	0.098	0.9953	0.061	0.102	0.2049	0.863
1,000	13.540	25.333	−0.080	0.8903	0.365	11.779	0.019	0.9963	0.046	0.796	0.9546	0.141

(c) Pseudo-first-order equation						(c) Pseudo-second-order equation				(c) Intraparticle diffusion equation		
C_0 (mg/L)	q (exp) (mg/g)	q_1 (mg/g)	k_1 (min^{-1})	$(R_1)^2$	MPSD	q_2 (mg/g)	k_2 g/(mg. min)	$(R_2)^2$	MPSD	K_3 (mg/(g min$^{1/2}$)]	$(R_3)^2$	MPSD
100	1.29	4.654	−0.002	0.1095	1.949	1.143	0.550	0.9983	0.021	0.018	0.1374	0.075
250	3.37	9.339	0.012	0.4714	0.517	3.153	0.412	0.9977	0.039	−0.063	0.6114	0.030
500	6.73	45.43	0.055	0.6918	3.690	5.452	0.075	0.9996	0.034	−0.176	0.9181	0.021
750	7.63	2.832	0.056	0.9022	2.557	7.806	0.481	0.9998	0.011	0.204	0.8276	0.035
1,000	8.85	5.015	0.067	0.9900	0.137	9.242	0.026	0.9999	0.008	0.316	0.8176	0.051

Table 10
Thermodynamic parameters for the adsorption of sulfide onto Fe–zeolite, Fe–Ag–zeolite and Ag–Cu–zeolite

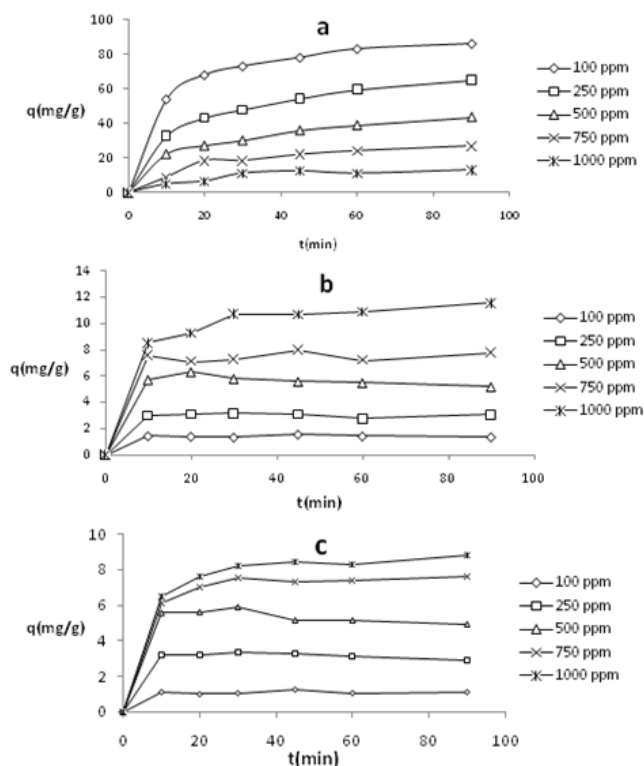| Zeolite	R^s	$\Delta H°$ (KJ/mol)	$\Delta S°$ (KJ/mol)	$\Delta G°$ (KJ/mol)			
				40°C	50°C	60°C	70°C
Fe	0.996	−7.43	−13.95	−2.57	−2.43	−2.30	−2.23
Fe–Ag	0.99	13.149	55.97	−3.765	−4.951	−5.444	−6.073
Ag–Cu	0.99	21.764	85.492	−5.063	−5.778	−6.632	−6.740

Fig. 4. Adsorption kinetics of sulfate onto (a) Fe–zeolite, (b) Fe–Ag–zeolite and (c) Ag–Cu–zeolite, at various initial sulfide concentration (conditions: particle size: –150 µm, speed stirrer: 500 rpm, 298 K temperature, pH: 11.5, amount of zeolite: 5 g).

Fe–Ag–zeolite and Ag–Cu–zeolite decreases, increases and increases, respectively.

3.6. Mechanism sulfide adsorption onto modified zeolite

Less report has been published so far toward an understanding of the mechanism of sulfide adsorption onto zeolite [51]. Of course, it has proposed some of the mechanisms of hydrogen sulfide onto various zeolites [52].

The mechanism of sulfide adsorption onto impregnation surface of zeolite depends on sulfide species form. It is therefore predicated that sulfide is absorbed in two cases: first the mechanism in solution pH > 10 in which the form of sulfide ion (S^{2-}) is predominated, and the adsorption process can occur via interacting to metal in the network of zeolite that is based on the formation of coordinative adsorbed species [53]. Of course, the tendency of transition metals to form coordination compounds confirms the following mechanism:

$$S^{2-} + M^+[ZeolO]^- \quad \rightarrow S^-......M^+[ZeolO]^- \qquad (7)$$

The second mechanism can be suggested in pH range of 5–10 which sulfide ions such as hydrogen sulfide (HS⁻) have formed in coordinative adsorbed [Eq. (7)], and the hydrogen bonding has occurred between the hydrogen of HS⁻ and oxygen atoms in the zeolite lattice, which contributes to adsorption process (Eqs. (8) and (9)). However, the tendency of transition metals to form coordination compounds confirms the above mechanism:

$$SH^- + [OZeol]^- M^+ \quad \rightarrow SH^-...... [OZeol]^-M^+ \qquad (8)$$

$$HS^- + M^+[ZeolO]^- \quad \rightarrow HS^-...... M^+[ZeolO]^- \qquad (9)$$

Of course, in this range of pH < 5, H_2S is formed, and through this mechanism with the participation of protons, a sulfur compound [53] will be formed (Eq. (10)):

$$SH_2 + [OZeol]^- M^+ \quad \rightarrow SH_2...... [OZeol]^- M^+ \qquad (10)$$

The improvement of sulfide adsorption on modified zeolite could be attributed to different parameters such as pore structure, the mobility of the ions in building the network construction, change of surface and characteristics of electrostatic interaction between fundamental groups of zeolite structure and modifier transition metals – sulfide ions. Modifier transition metals improved the adsorptive behavior of zeolite without changing its crystal structure.

In other words, the adsorption behavior of sulfide toward zeolite is affected by the location of metal ions in framework and lattice of zeolite. The more appropriate this place in zeolite structure is, the more synergism effect of metal ions on the electrostatic interaction between sulfide and metal ions will be, which causes the increase of sulfide adsorption.

4. Conclusions

These findings have shown that the best-modified zeolites were synthesized by using the Fe(III), Fe(III)–Ag(I) and Ag(I)–Cu(II) salts. The synergism effect of a mixture of modified salt metals on the sulfide adsorption was obviously observed.

The value of adsorbed sulfide onto modified zeolite was influenced by solubility product constant (K_{sp}) of transition metal sulfides. The best-modified zeolite relates to Fe–Ag–zeolite that due to their lowest K_{sp} of Ag_2S and Fe_2S_3 sis relative to K_{sp} of other transitional metals sulfide, which have been applied in this study. There was no observation of the appreciable change in the XRD patterns Fe–zeolite, Fe–Ag–zeolite, and Ag–Cu–zeolite after modifying treatment, which does not indicate any crystal structural change with loading transitional metals on Iranian zeolite. No significant change vibration band of functional groups of modified zeolite was observed. In other words, Fe(III), Ag(I) and Cu(II) ions impregnated surface of zeolite (clinoptilolite).

It was found that the Langmuir isotherm model describes well the sulfide adsorption onto Fe–zeolite and Ag–Cu–zeolite adsorbents. It shows that homogeneous (monolayer surface) adsorption and the reversible process are predominant. With respect to S.D. and regression coefficients (R^2) values of Langmuir, Freundlich and Temkin isotherm model for Fe–Ag–zeolite are similar to each other. It seems the complexity treatment is predominant in this adsorption.

The maximum capacity of sulfide adsorption relates to Ag–Fe–zeolite, which was confirmed by the value of the specific surface area of Ag–Fe–zeolite. The magnitude of E (free energy of adsorption) illustrated that adsorption characteristics for Fe–zeolite, Fe–Ag–zeolite and Ag–Cu–zeolite include chemical absorption ion-exchange process, physically process and physically process, respectively. Analysis of

the kinetics revealed that the pseudo-second-order-sorption mechanism is predominant.

The kinetic study adsorption of sulfide onto modified zeolite demonstrates that the experimental data fitted the pseudo-second-order kinetics well. In other words, it means that both concentration adsorbate (sulfide ions) and the number of active sites of modified zeolite have affected adsorption mechanism and the rate of adsorption.

The calculated thermodynamic parameters of sulfide adsorption onto modified zeolite reveals the negative $\Delta G°$ values at different temperatures indicating that the adsorption process is spontaneous but for Fe–zeolite become less negative with the increase of temperature indicating that sulfide adsorption is exothermic (negative $\Delta H°$). The positive $\Delta H°$ value of sulfide adsorption onto Fe–Ag–zeolite and Ag–Cu–zeolite indicates that the adsorption was endothermic. The negative value of $\Delta S°$ indicates that sulfide adsorption onto Fe–zeolite is an associative process. The positive value of changes in standard entropy occurs as a result of the redistribution of energy between the sulfide and both adsorbents (Fe–Ag–zeolite and Ag–Cu–zeolite). Based on the results of this paper, it can be concluded that the Fe–zeolite, Fe–Ag–zeolite and Ag–Cu–zeolite are appropriate adsorbents for removing sulfide ions from aqueous solution, and it is introduced as new materials for wastewater treatment.

References

[1] H.R. Mortaheb, F. Ghaemmaghami, B. Mokhtarani, A review on removal of sulfur components from gasoline by pervaporation, Chem. Eng. Res. Des., 90 (2012) 409–432.

[2] L. Altas, H. Buyukgungor, Sulfide removal in petroleum refinery wastewater by chemical precipitation, J. Hazard. Mater., 153 (2008) 462–469.

[3] A. Al-Haddad, E. Azrag, A. Mukhopadhyay, Treatment experiments for removal of hydrogen sulfide from saline groundwater in Kuwait, Desal. Wat. Treat., 52 (2014) 3312–3327.

[4] T.J. Bandosz, On the adsorption/oxidation of hydrogen sulfide on activated carbons at ambient temperatures, J Colloid Interface Sci., 246 (2002) 1–20.

[5] X. Xu, C. Chen, A. Wang, Simultaneous removal of sulfide, nitrate and acetate under denitrifying sulfide removal condition: modeling and experimental validation, J. Hazard. Mater., 264 (2014) 16–24.

[6] P.K. Dutta, K. Rabaey, Z. Yuan, Spontaneous electrochemical removal of aqueous sulfide, Water Res., 42 (2008) 4965–4975.

[7] C.M. Silva, P.F. Lito, J.P.S. Aniceto, Removal of anionic pollutants from waters and wastewaters and materials perspective for their selective sorption, Water Air Soil Pollut., 223 (2012) 6133–6155.

[8] A. Dar, U. Shafique, J. Anwar, Removal of sulfide ions from water using rice husk, J. Sulfur Chem., 36 (2015) 187–195.

[9] S. Hokkanena, E. Repoa, A. Bhatnagarb, Adsorption of hydrogen sulphide from aqueous solutions using modified nano/micro fibrillated cellulose, Environ. Technol., 18 (2014) 2334–2346.

[10] P. Cosoli, M. Ferrone, S. Pricl, Hydrogen sulfide removal from biogas by zeolite adsorption, Part II. MD simulations, Chem. Eng. J., 145 (2008) 93–99.

[11] M. Jiang, F.T. Ng, Adsorption of benzothiophene on Y zeolites investigated by infrared spectroscopy and flow calorimetry, Catal. Today, 116 (2006) 530–536.

[12] S. Yaşyerli, I. Ar, G. Doğu, T. Doğu, Removal of hydrogen sulfide by clinoptilolite in a fixed bed adsorber, Chem. Eng. Process. Process Intensif., 41 (2001) 785–792.

[13] M. Pigna, A. Violante, Adsorption of sulfate and phosphate on Andisols, Commun, Soil Sci. Plant Anal., 34 (2003) 2099–2113.

[14] A. Kuleyin, Removal of phenol and 4-chlorophenol by surfactant-modified natural zeolite, J. Hazard. Mater., 144 (2007) 307–315.

[15] M. Ishiguro, T. Makino, Sulfate adsorption on a volcanic ash soil (allophanic Andisol) under low pH conditions, Colloids Surf. A., 384 (2011) 121–125.

[16] M. Montazerolghaem, A, Rahimi, F. Seyedeyn-Azad, Equilibrium and kinetic modeling of adsorptive sulfur removal from gasoline by synthesized Ce–Y zeolite, Appl. Surf. Sci., 257 (2010) 603–609.

[17] A. Alonso-Vicario, J.R. Ochoa-Gómez, S. Gil-Río, O. Gómez-Jiménez-Aberasturi, C. Ramírez-López, J. Torrecilla-Soria, A. Domínguez, Purification and upgrading of biogas by pressure swing adsorption on synthetic and natural zeolites, Microporous Mesoporous Mater., 134 (2010) 100–107.

[18] W. Chen, H.-c. Liu, Adsorption of sulfate in aqueous solutions by organo-nano-clay: adsorption equilibrium and kinetic studies, J. Cent. South Univ., 21 (2014) 1974–1981.

[19] B. Erdog, M. Sakızcı, E. Yorukogullar, Characterization and ethylene adsorption of natural and modified clinoptilolites, Appl. Surf. Sci., 254 (2008) 2450–2457.

[20] P. Misaelides, Application of natural zeolites in environmental remediation: a short review, Microporous Mesoporous Mater., 144 (2011) 15–18.

[21] G.M. Haggerty, R.S. Bowman, Sorption of chromate and other inorganic anions by organo-zeolite, Environ. Sci. Technol., 28 (1994) 452–458.

[22] P. Chutia, S.H. Kato, T. Kojima, Adsorption of As(V) on surfactant-modified natural zeolites, J. Hazard. Mater., 162 (2009) 204–211.

[23] S. Velu, X.I. Ma, C.H. Song, Selective adsorption for removing sulfur from jet fuel over zeolite-based adsorbents, Ind. Eng. Chem. Res., 42 (2003) 5293–5304.

[24] Y.W. Li, F.H. Yang, G.S. Qi, Effects of oxygenates and moisture on adsorptive desulfurization of liquid fuels with Cu(I)Y zeolite, Catal. Today, 116 (2006) 512–518.

[25] J. Liao, W. Bao, Y. Chen, The adsorptive removal of thiophene from benzene over ZSM-5 zeolite, Energy Sources Part A, 34 (2012) 618–625.

[26] S. Velu, C. Song, M.H. Engelhard, Adsorptive removal of organic sulfur compounds from jet fuel over K-exchanged NiY zeolites prepared by impregnation and ion exchange, Ind. Eng. Chem. Res., 44 (2005) 5740–5749.

[27] A.E. Ofomaja, Y. Ho, Equilibrium sorption of anionic dye from aqueous solution by palm kernel fibre as sorbent, Dyes Pigm., 74 (2007) 60–66.

[28] M. Özacar, A. Şengil, Equilibrium data and process design for adsorption of disperse dyes onto alunite, Environ. Geol., 45 (2004) 762–768.

[29] E. Bulut, M. Özacar, A. Şengil, Adsorption of malachite green onto zeolite: equilibrium and kinetic studies and process design, Microporous Mesoporous Mater., 115 (2008) 234–246.

[30] V.C. Srivastava, I.D. Mall, I.M. Mishra, Antagonistic competitive equilibrium modeling for the adsorption of ternary metal ion mixtures from aqueous solution onto bagasse fly ash, Ind. Eng. Chem. Res., 47 (2008) 3129–3137.

[31] K.Y. Foo, B.H. Hameed, Insights into the modeling of adsorption isotherm systems, Chem. Eng. J., 156 (2010) 2–10.

[32] Y.S. Ho, C.T. Huang, H.W. Huang, Equilibrium sorption isotherm for metal ions on tree fern, Process Biochem., 37 (2002) 1421–1430.

[33] Y.S. Ho, Removal of copper ions from aqueous solution by tree fern, Water Res 37 (2003) 2323–2330.

[34] J. Mendham, Vogels Textbook of Quantitative Chemical Analysis, Pearson Education India, 2006.

[35] R.J. Tayade, R.G. Kulkarni, R.V. Jasra, Transition metal ion impregnated mesoporous TiO$_2$ for photocatalytic degradation of organic contaminants in water, Ind. Eng. Chem. Res., 45 (2006) 5231–5238.

[36] C.P. Saha, R.J. Wakeman, Sorption of atrazine on conventional and surface modified activated carbons, J. Colloid Interface Sci., 302 (2006) 408–416.

[37] G. Tan, D. Xiao, Adsorption of sulfide ion from aqueous solution by ground wheat stems, J. Hazard. Mater., 164 (2009) 1359–1363.

[38] G. Crini, N. Harmel, C. Robert, Removal of C.I. Basic Green 4 (Malachite Green) from aqueous solutions by adsorption using cyclodextrin-based adsorbent: kinetic and equilibrium studies, Sep. Purif. Technol., 53 (2007) 97–110.

[39] N. Öztürk, T. Ennil Bektaş, Nitrate removal from aqueous solution by adsorption onto various materials, J. Hazard. Mater., 112 (2004) 155–162.

[40] R. Huang, B. Wang, B. Yang, Equilibrium, kinetic and thermodynamic studies of adsorption of Cd(II) from aqueous solution onto HACC–bentonite, Desalination, 280 (2011) 297–304.

[41] M.I. Tempkin, V. Pyzhev, Kinetics of ammonia synthesis on promoted iron catalyst, Acta Physiochim. USSR, 12 (1940) 327–356.

[42] M. Özacar, A. Şengil, A kinetic study of metal complex dye sorption onto pine sawdust, Process Biochem., 40 (2005) 565–572.

[43] I.D. Mall, V.C. Srivastava, N.K. Agarwal, Removal of congo red from aqueous solution by bagasse fly ash and activated carbon: Kinetic study and equilibrium isotherm analyses, Chemosphere, 61 (2005) 492–501.

[44] M. Doğan, M. Alkan, Ö. Demirbaş, Adsorption kinetics of maxilon blue GRL onto sepiolite from aqueous solutions, Chem. Eng. J., 124 (2006) 1–3.

[45] M.M. Dubinin, L.V. Radushkevich, The equation of the characteristic curve of the activated charcoal, Proc. Acad. Sci. USSR Phys. Chem. Sect., 55 (1947) 331–337.

[46] Y. Ho, Citation review of Lagergren kinetic rate equation on adsorption reactions, Scientometrics, 59 (2004) 171–177.

[47] M. Özacar, Equilibrium and kinetic modelling of adsorption of phosphorus on calcined alunite, Adsorption, 9 (2003) 125–132.

[48] M. Özacar, A. Şengil, Application of kinetic models to the sorption of disperse dyes onto alunite, Colloids Surf. A, 242 (2004) 105–113.

[49] K.R. Scheckel, L. Donald, Sparks temperature effects on nickel sorption kinetics at the mineral–water interface, Soil Sci. Soc. Am. J., 65 (2001) 719–728.

[50] M. Karatas, Removal of Pb(II) from water by natural zeolitic tuff: kinetics and thermodynamics, J. Hazard. Mater., 199–200 (2012) 383–389.

[51] G. Sethia, R.S. Somani, H. Chand Bajaj, Adsorption of carbon monoxide, methane and nitrogen on alkaline earth metal ion exchanged zeolite-X: structure, cation position and adsorption relationship, RSC Adv., 5 (2015) 12773–12781.

[52] M. Ozekmekci, G. Salkic, M. Ferdi Fellah, Use of zeolites for the removal of H_2S: a mini-review, Fuel Process. Technol., 139 (2015) 49–60.

[53] M. Ziolek, M. Sugioka, Adsorption and dehydrosulfurization of aliphatic thiols on zeolites, Res. Chem. Intermed., 26 (2000) 358–412.